# Experimental Analysis into the Effects of Air Compressibility in OWC Model Testing

Damon Howe[#1], Jean-Roch Nader[#2], Gregor Macfarlane[#3]

[#] *National Centre for Maritime Engineering & Hydrodynamics, Australian Maritime College, University of Tasmania*
*Locked Bag 1395, Launceston, Tasmania 7250, Australia*

[1]damon.howe@utas.edu.au

[2]JeanRoch.Nader@utas.edu.au

[3]gregorm@amc.edu.au

**It is well documented that the effect of air compressibility will potentially influence the performance of an Oscillating Water Column (OWC) device, with a number of previous theoretical studies examining these effects [1-5]. The implications of air compressibility have the most significant effect at full scale, which can be attributed to the large air chamber volume and the increase in associated pressure and flow rate. However, the development of wave energy converter technology relies significantly on model scale testing, which is often scaled using the Froude criterion. This scaling method are not appropriate for the modelling of air compressibility and introduces uncertainties in the prediction the performance results at full-scale. To account for these effects, methods have been derived to more accurately represent the effect of air compressibility at small scale, one of which requires scaling the air chamber volume by the scale factor squared as opposed to the traditional scale factor cubed following the Froude criterion methodology [1]. This paper examines a preliminary investigation into the effect of air compressibility through hydrodynamic experimentation of a bent duct OWC device, from which the behaviour of the obtained results are compared with the expression proposed analytically by Sarmento and Falcao [1].**

***Keywords*— Oscillating Water Column, Wave Energy Converter, Air Compressibility, Hydrodynamic Experimentation**

## I. Introduction

A number of reviews have been transcribed that detail the current status of ocean renewable energy, from technological, economical and resource availability perspectives such as in [6-15] to present a few. Pivotal to concept development of ocean renewable energy technologies is model scale hydrodynamic experimentation of devices, and the relevant interpretations and conclusion concerning the corresponding full-scale device characteristics. Model scale testing offers an economical platform for concept validation, and provides a pivotal step in the procession of a technology through the Technology Readiness Levels (TRLs) [16].

With reference to technology maturity, the Oscillating Water Column (OWC) Wave Energy Converter (WEC) is recognised as the most tested and developed, whilst also being one of the most promising and simplistic technologies for ocean wave energy extraction. The OWC WEC also offers the largest contingent of full-scale devices, predominantly pre-commercial in their deployment (see [17-21]). Many device variations have been conceptualised and tested at model scale covering both isolated and breakwater integrated devices, exploring features from vortex generation reduction through to device performance [22-28]. Although advancements have been made in testing facility capabilities, along with the development of concept testing guidelines [29], there are still a number of issues related to the experimentation of these devices due to the difficulty scaling the Power Take-Off (PTO) system and the corresponding difficulty associated with air compressibility at small scale.

One major research and development aspect identified by Falcao et al. is the potential discrepancies associated with the inflow and outflow processes of air through the Power Take-Off (PTO) system [4]. The complex mixing of the de-pressurised lower density air within the chamber with external atmospheric air during inflow can result in thermal changes of the air, subsequently resulting in air compressibility. This factor can have both positive and negative impacts on the performance of the device [30, 31], and a number of systems have been designed to either mitigate or alleviate this phenomena, including latching-control mechanisms as in [2] and also pressure release valves which have recently been investigated by Wave Swell Energy for their bottom mounted nearshore device [26].

As gravitational and inertial forces tend to be the dominant forces in hydrodynamics, model scale testing is typically undertaken using the Froude criterion. One focal uncertainty associated with air compressibility is its inability to be effectively scaled using the Froude criterion. With wave basin experiments being of such crucial importance in the development of WEC technology, the absence of air compressibility can result in misleading performance evaluation at the model scale, hence unreliable prediction of full-scale performance as described by Elhanafi et al in [32].

A method has been derived in an attempt to account for the effects of air compressibility during wave basin tests of WECs, in which Sarmento and Falcao propose that the full-scale air chamber volume be scaled by the scale-factor ($\lambda$) squared. This method is opposed to scaling by the scale factor cubed which is typically associated for volumetric scaling under the Froude criterion [1, 5].

This paper details a preliminary investigation into effect of air compressibility through hydrodynamic experimentation of a bent duct type OWC device at 1:20 scale conducted in shallow water wave basin. The behaviour of the results obtained are analysed and compared with the analytically derived

expression proposed by Sarmento and Falcao [1]. Based on the alternate methodology for air chamber scaling proposed by Sarmento and Falcao ($\lambda^2$), the OWC model would require an air chamber volume around 0.5 m$^3$. The volumetric variations investigated here varies from no additional volume (corresponding to previous studies using this device [22-24]), through to an additional 1.5 m$^3$ of volume, with 0.5 m$^3$ increment.

A thin-walled bent duct type OWC WEC facing towards the incoming incident wave propagation is considered for the experimental investigation. The surface piercing device operates in constant water depth $h$. The device in designed having an inlet width $W_D$, inlet height $H_D$, and thickness $t_D$, highlighted in Fig. 1.

## II. Theory

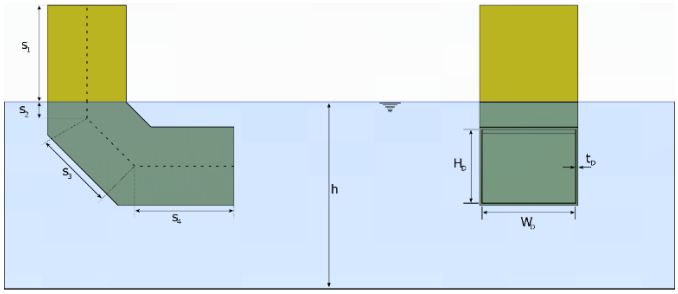


Fig. 1 Schematic diagram of OWC device detailing front and side views. The chamber chord length correlates to the sum of the variables $s_1$, $s_2$, $s_3$ and $s_4$.

### A. Theoretical Hydrodynamic Consideration

The propagating monochromatic incident plane wave travels towards the OWC device with amplitude $\eta_0$ and frequency $\omega$. Linear water-wave theory is assumed, whilst considering irrotational and inviscid flow.

As interaction between incident waves and the OWC device occurs, a volume flux $Q$ is generated within the chamber, which when interacting with the PTO system, creates a dynamic pressure $P_c$ that oscillates around the mean atmospheric pressure. Following Sarmento and Falcao [1], a linear relationship between $p_c$ and $q$ (complex forms of $P_c$ and Q in the frequency domain) is considered for the PTO system damping, which is typically associated with a Wells turbine. This relationship is written in the frequency domain as,

$$q = \left(\gamma_r - i\gamma_c\right) p_c \tag{1}$$

where,

$$\gamma_r = \frac{KD_t}{N\rho_{0,a}} \tag{2}$$

$K$ is the empirical turbine coefficient based on the design, number of and set up of the turbines, $D_t$ is the turbine diameter, $N$ is the rotational speed of the turbine and $\rho_{0,a}$ is air density, and

$$\gamma_c = \frac{\omega V_{0,c}}{c_a^2 \rho_{0,a}} \tag{3}$$

where, $V_{0,c}$ is the chamber volume and $c_a$ is the velocity of sound in air.

### B. Experimental Hydrodynamic Consideration

When considering the total volume flux from an experimental standpoint, it can be express as follows,

$$Q = \iint_{S_c} \frac{\partial \eta}{\partial t} ds = \iint_{S_c} v_s ds = \bar{v}_s S_c \tag{4}$$

where $v_s$ represents the velocity of the free surface, $S_c$ is the cross sectional area of the chamber and $\bar{v}_s$ is the average velocity under the assumption the free surface will move uniformly.

Considering the performance of the device, the instantaneous power at a given time $t$, is derived as,

$$P\left(t\right) = P_c Q \tag{5}$$

where $P$ is power in Watts. The mean hydrodynamic power absorbed over a given wave period is equated as,

$$P_h = \frac{1}{T}\int_0^T P_c Q \quad dt \tag{6}$$

where $P_h$ is the mean absorbed hydrodynamic power and $T$ is the wave period.

With reference to Equation (1),

$$\gamma = \left\|\gamma\right\| e^{i\varphi_\gamma} = \gamma_r - i\gamma_c \tag{7}$$

where $\varphi_\gamma$ represents the phase, found as,

$$\varphi_\gamma = \varphi_Q - \varphi_{p_c} \tag{8}$$

where $\varphi_Q$ represents the phase of the volume flux, and $\varphi_{pc}$ represents the phase of the dynamic pressure. The hydrodynamic coefficients are determined experimentally using the amplitude of pressure and volume flux.

$$\left\|\gamma\right\| = \frac{ampl(Q)}{ampl(p_c)} \tag{9}$$

Finally, the capture width, $L_{pc}$, is defined as,

$$L_{pc} = \frac{P_h}{\frac{1}{2}\rho g C_g \eta_0^2} \tag{10}$$

where $\rho$ is the water density, $g$ is gravitational acceleration and $C_g$ is group velocity.

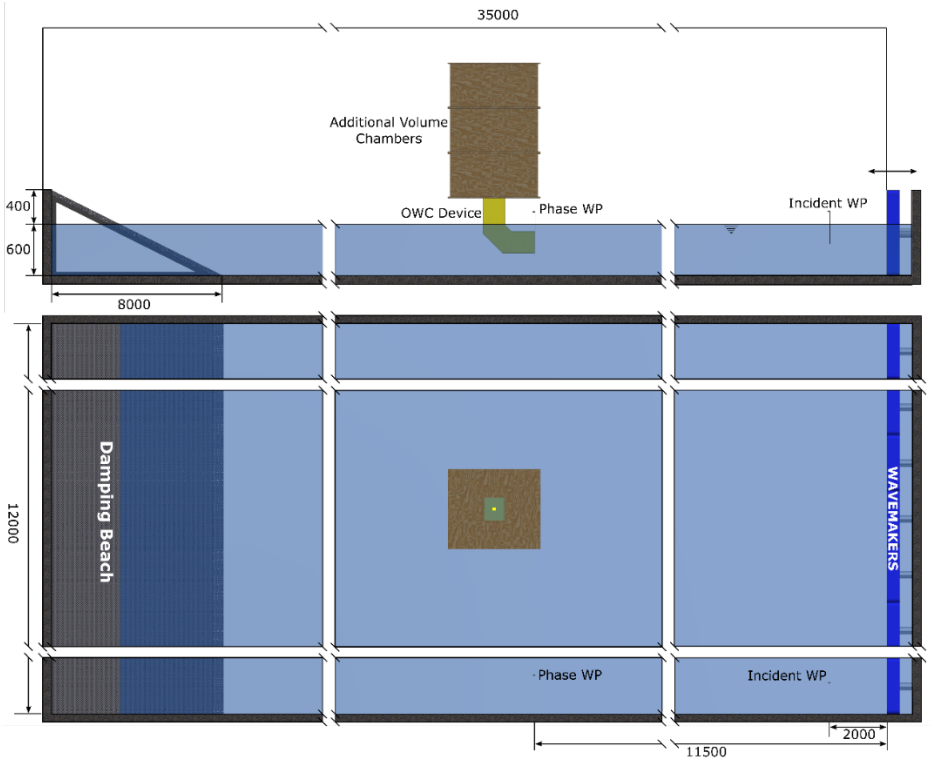


Fig. 2 Side and top view of the experimental configuration within the AMC Model Test Basin, all units in mm (not to scale).

## III. Methodology

### A. Experimental Considerations

1) *Pneumatic Damping*: To simulate the desired linear damping relationship between dynamic chamber pressure and total volume flux, a porous fabric mesh termed Enviro-Cloth was sealed to the chamber outlet to provide a PTO representation at model scale, as previously used in [22-24]. The previous methodology to establish the pneumatic damping coefficient is outlined in [22], which includes the sources of error associated with the required numerical derivations. It should be noted that the mass-flow rate through the Enviro-Cloth as a function of the pressure difference between internal dynamic pressure and atmospheric pressure obeys the approximately linear relationship as proposed in [1].

### B. Model Test Basin

The experimental investigation was conducted in the Australian Maritime College's 35 m long × 12 m wide × 1 m maximum depth Model Test Basin. The facility houses a multi-element piston-type wavemaker capable of producing both regular and irregular waveforms. The basin also incorporates a damping beach at the opposite end of the basin to dissipate the systems energy. A schematic of the experimental configuration within the basin is illustrated in Fig. 2.

### C. Physical Model

The OWC model utilised for the experimental investigation is a 1:20 scale device having rectangular cross-sectional geometry, which has previously been employed for various hydrodynamic experimentation as in [22-24]. Alterations to the design of the device were conducted to incorporate a separate but directly linked receptacle to increase the OWC air chamber volume.

The variable air chamber volume model was devised to incorporate three identical compartments, which could be incrementally combined to increase the air volume methodically throughout the experimental investigation. The connection of the additional air compartments and the OWC device was achieved through a specifically designed adapter plate, which allowed an airtight seal to be maintained between the device and the additional compartments. Each compartment was designed to have a specific volume corresponding to 0.5 cubic metres, subsequently the air chamber volume variations tested were 0.5, 1 and 1.5 cubic metres of additional volume. The additional compartments were constructed of 12 mm plywood, and sealed with an epoxy coating to create an impermeable layer. Each compartment had a 70 mm top and bottom flange utilised in the connection of the modular units, which were clamped together to compress an 8 mm × 13 mm rubber gasket to maintain airtightness.

The compartments had a 0.23 m × 0.3 m opening at the top and bottom symmetrical about the longitudinal and transverse midpoint. These openings corresponded to the dimensions of the device outlet cross-section, and were utilised for the purpose of connection and as an outlet to which the PTO damping simulant could be applied as shown in Fig. 3.

Fig. 3 Model scale OWC device fitted with additional 1.5 m3 air chamber (left), 1 m3 air chamber (middle) and PTO simulant secured using sealing plate (right)

### *D. Instrumentation and Calibration*

To measure the performance of the OWC device, along with the accuracy of the desired incident wave train, a series of resistance-type wave probes, and a Honeywell Controls TruStability board mount pressure sensor were utilised throughout the experimental investigation. The pressure sensor was configured with the OWC device through a small pressure tap located on the side of the device and was connected to an Ocean Controls KTA-284 instrumentation amplifier to increase the data quality.

The three wave probes were configured as an incident, phase and internal OWC probe respectively, having locations within the wave basin corresponding to those presented in Fig. 2.

All probes were calibrated daily to reduce the uncertainties associated with daily changes to the facility environment. Calibration and sensitivity data can be found in Table I.

TABLE I
SENSOR PROPERTIES

| Sensor | Range | Sensitivity | Output |
|---|---|---|---|
| Wave - Incident | ± 40 mm | 0.25 VDC/mm | ±10 VDC |
| Wave - Phase | ± 40 mm | 0.25 VDC/mm | ±10 VDC |
| Wave - OWC | ± 60 mm | 0.167 VDC/mm | ±10 VDC |
| Pressure - OWC | ± 400 Pa | 25 mVDC/Pa | ±10 VDC |

### *E. Experimental Test Regime*

The experimental test regime investigated four separate air chamber volume variations. Each volumetric variation of the device was subjected to 20 mm height across a frequency bandwidth of 0.4 Hz - 1.2 Hz, with the results obtained processed using phase averaging, a technique previously employed in analysing model scale hydrodynamic experimental data [22-24, 33, 34]. The frequency increment resolution was increased around resonance to provide better detail of the device performance at resonance.

### *F. Data Processing*

As with previous experimental investigations associated with bent duct type model scale OWC devices, the phase averaging data post processing technique was employed to accurately evaluate the performance of the OWC conditional variations [22-24, 33-36]. Orphin *et al.* conducted a suite of experiments investigating the uncertainty associated with model scale hydrodynamic experimental testing of an OWC device where they concluded that that results obtained via phase averaging are within ± 2% of the results obtained from 10 identical repeat runs [24]. The methodology followed is the same as that outlined in [22], from which the processed data was then utilised to derive the measurements of interest pertaining to the volumetric and damping variations.

## IV. RESULTS AND DISCUSSION

### *A. Pneumatic Damping Coefficient, δ*

As previously addressed, a linear damping relationship for the model scale PTO substitute was desired for the hydrodynamic testing. Previous evaluations of Enviro-Cloth fabric mesh as a PTO simulant yielded results that indicated its ability to provide linear damping characteristics at model scale [22-24]. With these characteristics in mind, the fabric mesh was applied identically across the four volumetric variations of the OWC air chamber to establish how additional air chamber volume influences the linearity of the damping, and the relationship between pressure and volume flux within the chamber.

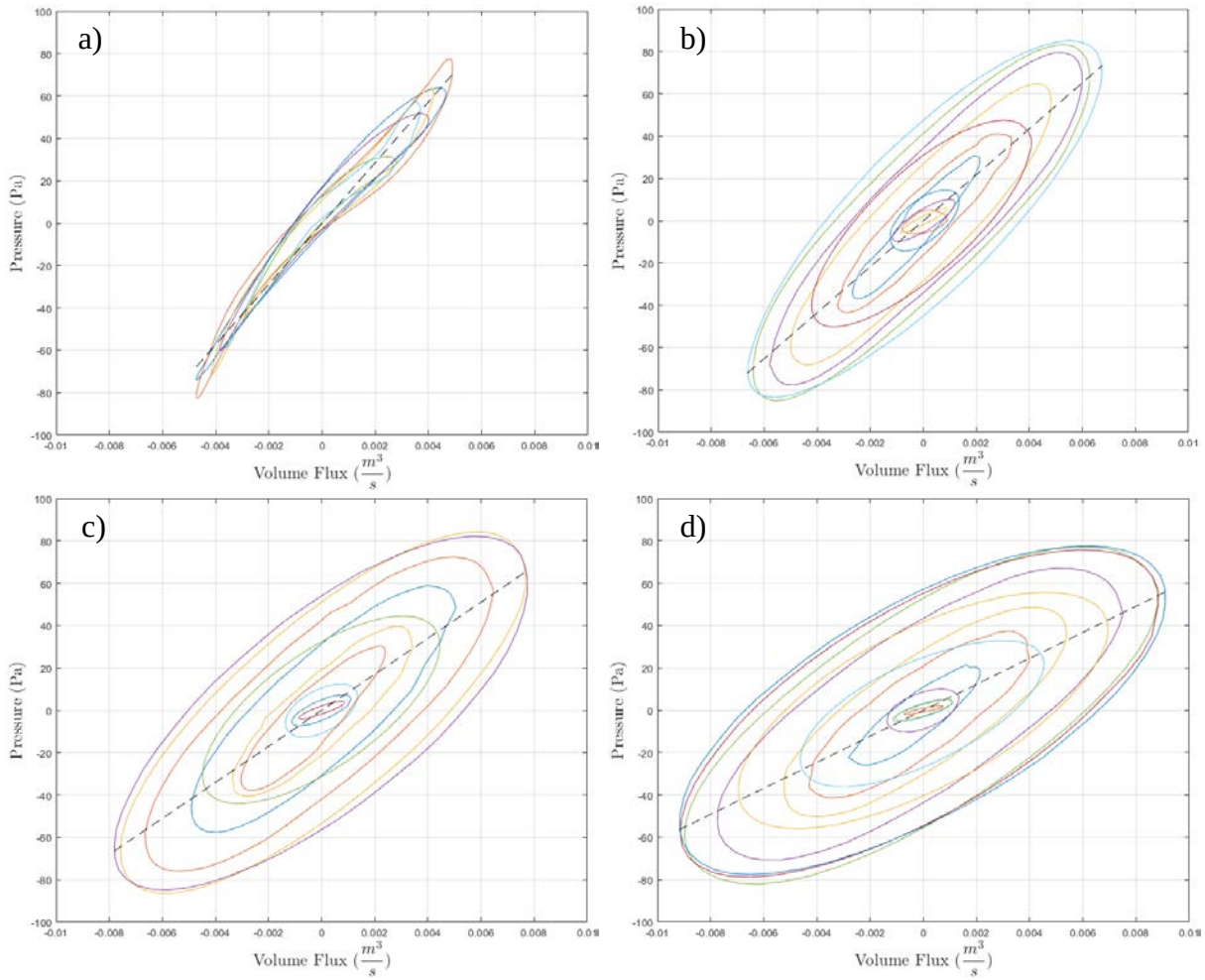


Fig. 4 Damping relationship between pressure and volume flux for increasing chamber volumes: a) No additional volume b) 0.5 $m^3$ additional volume c) 1.0 $m^3$ additional volume d) 1.5 $m^3$ additional volume.

Fig. 4 illustrates the pneumatic damping characteristics of the OWC PTO simulant as the air chamber volume increases. Fig. 4a displays the typical damping relationship previously established for the unaltered OWC device in isolation, where it is illustrated that for all experimental incident wave frequencies (characterized by contrasting coloured lines) that an approximate linear relationship can be assumed, defined by the dashed line. Further investigating Fig. 4a, it can be recognised that the effects of air compressibility are not conclusive due to the lack of observable phase shift between the pressure and volume flux data. This is most easily observed at the local maxima and minima for pressure, where the corresponding maxima and minima for volume flux are also observable. For this case, which also represents a large portion of experimental testing of OWC devices, the air-compressibility is usually overlooked. It should be however noted that the apparent hysteresis visible in Fig. 4a is associated with a pressure leak at the outlet of the chamber. Subsequently the results obtained for $\gamma_r$, $\gamma_c$ and $\tilde{L}_{pc}$. for the no added volume are considered erroneous and are not presented in the following.

As the volume of the OWC air chamber incrementally increases (0.5 $m^3$, 1 $m^3$ and 1.5 $m^3$ in Fig. 4b, 4c and 4d respectively), the effects of air compressibility become apparent, as a phase shift is clearly discernible between the internal pressure and volume flux as the corresponding maxima and minima are unaligned. The linear regression to obtain the pneumatic damping coefficient cannot be applied for these cases. It should also be noted that the relationship between $P_c$ and $Q$ seems to change with frequency.

In order to further investigate the air compressibility effect, $\gamma_r$ and $\gamma_c$ were derived using Equation (7-9).

### B. *Compressibility Coefficient, $\gamma_c$*

Analysis of the hydrodynamic components of the pneumatic damping is presented in which detail the compressibility against frequency and against different air chamber volumes, $V_{0,c,}$ and turbine coefficients respectively.

First investigating the compressibility coefficient, $\gamma_c$, in Fig. 5, the coefficient is plotted for the different air chamber volumes, $V_{0,c}$, on the x-axis and different frequencies represented by the colour markers. In Fig. 6, the coefficient is plotted for the different frequencies on the x-axis and the air chamber volumes, $V_{0,c}$, are represented by the colours markers. Analysing the result, the value of the compressibility

coefficient is seen to increase with respect to both $V_{0,c}$, and $f$ the incident wave frequency. A linear trend seem to appear in the data in both Fig. 5 and Fig. 6, which corresponds correctly with the expected outcomes governed by Equation (3).

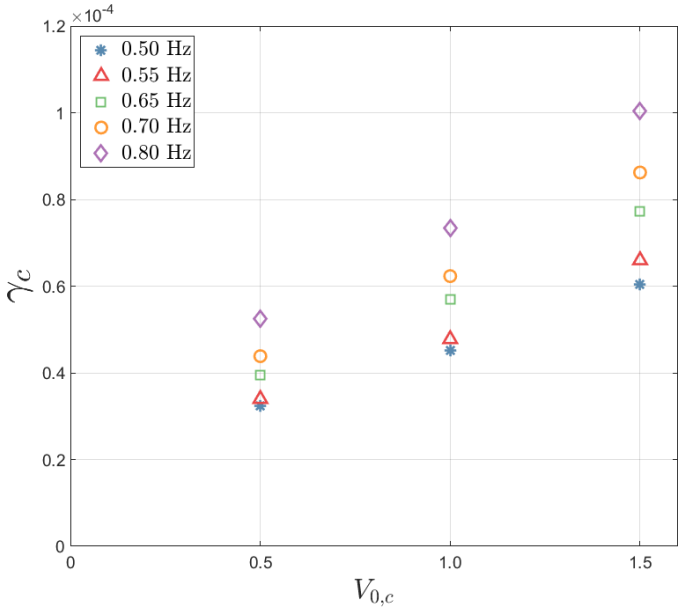


Fig. 5 Compressibility coefficient, $\gamma_c$, with respect to volumetric and incident wave frequency increases

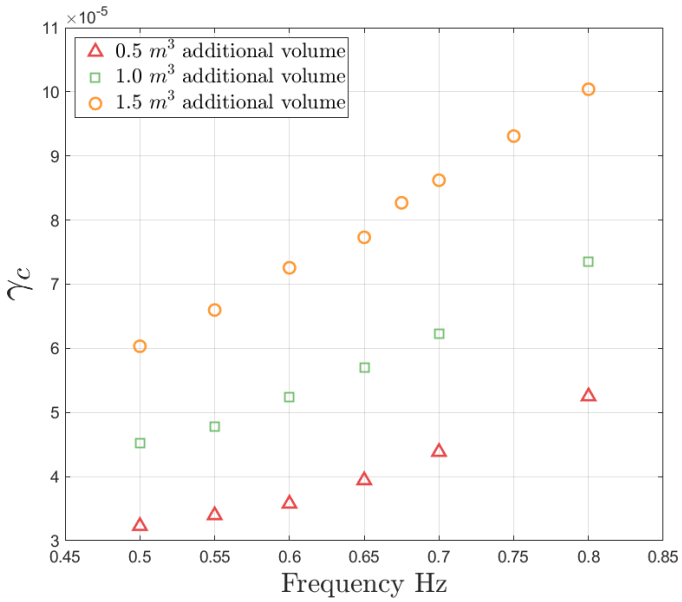


Fig. 6 Compressibility coefficient, $\gamma_c$, with variations of incident wave frequency for varying volume cases.

Rewriting Equation (3) in the form of

$$\gamma_c = C\left(\omega V_{0,c}\right) + k \tag{11}$$

the values of $C$ and $k$ where derived using the experimental data and presented in Table II for the different $V_{0,c}$ and compare with its theoretical value.

TABLE II
$C$ AND $K$ VALUE FOR VOLUMETRIC VARIATIONS

| Volume ($m^3$) | Experimental $C$ ($10^{-4}$) | Theoretical $C$ ($10^{-4}$) | Experimental $k$ ($10^{-4}$) |
|---|---|---|---|
| 0.5 | 0.0926 | | 0.1724 |
| 1.0 | 0.0928 | 0.0694 | 0.2004 |
| 1.5 | 0.0953 | | 0.2758 |

Previous hydrodynamic experimentation from the authors was able to establish that for small values of $V_{0,c}$ the value of $\gamma_c$ will be very close to zero, subsequently resulting in no discernible phase shift between the volume flux and dynamic pressure [22]. In the same way, as the incident wave frequency tends toward zero, indicating still water conditions, the value for $\gamma_c$ will also be zero. This correlates correctly to the theoretical expression derived by Sarmento and Falcao [1] which tends toward zero as both volume and frequency tend towards zero.

The results illustrated in Fig. 5, Fig. 6 and Table II indicate a disparity from the theoretical expression. It was established that as $V_{0,c}$ and $\omega$ tend away from zero, the data followed a relationship defined by the newly derived expression presented in Equation (11). The value for $C$ remains relatively constant throughout the volumetric air chamber variations tested, but is different from the theoretical value proposed, as found in Table II. Similarly, the newly derived expression presents the coefficient $k$, which appears to be a function of volume, as such can be considered dependent upon the value of $V_{0,c}$.

As illustrated in Fig. 5 and Fig. 6, a key finding from the experimental investigation was the linearity of the relationship between $\gamma_c$ and both $V_{0,c}$ and $\omega$ respectively. This provides evidence indicating the trend adheres to the linearity of the theoretical expression, which provides a promising foundation for future development. The variation in the magnitude of the slope, and subsequent introduction of the coefficient $k$ indicates that revision of the theoretical model should be investigated at full scale and verified through experimental measures to provide greater understanding of the influence of air compressibility in large scale devices.

The linearity of the established relationships in culmination with further development of the theoretical model provides a platform that can be developed further into a methodology for better simulating the PTO system and air compressibility effects at model scale.

It should be noted that the highly dynamic environment within the OWC chamber associated with the natural resonant frequency of the device did not have any apparent effect on the results presented in Fig. 5 and Fig. 6 where the natural resonance frequency of the device was found around 0.55 Hz.

### C. Turbine Coefficient, $\gamma_r$

The second of the hydrodynamic coefficients related to the pneumatic damping imposed on the system by the PTO simulant is the turbine coefficient, $\gamma_c$. Fig. 7 illustrates the results obtained from experimental testing against the frequencies on the x-axis and the air chamber volumes, $V_{0,c}$, are represented by the colours markers.

$\gamma_r$ is found to stay relatively constant over the frequencies, well within the uncertainties related to the measurements. One key outcome, however, is the dependence of $\gamma_r$ with the air chamber volumes, $V_{0,c}$. Although the damping on the orifice simulated by the layers of enviro-cloth were the same, $\gamma_r$ increases with $V_{0,c}$ which does not follow the expected outcome from Equation (2). In practice, $\gamma_r$ can nevertheless be altered by changing the number of Enviro-Cloth layers utilised for the PTO simulant.

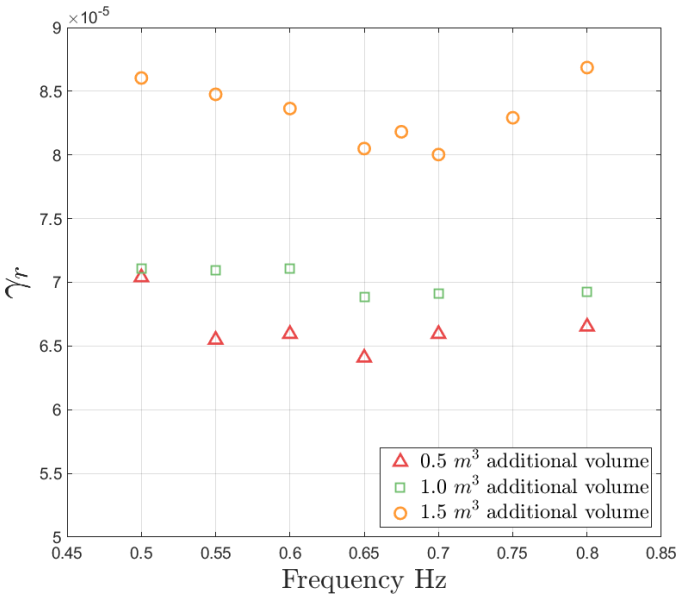


Fig. 7 Turbine coefficient, $\gamma_r$, for variations in incident wave frequency across tested volumetric variations.

The results displayed in this section can have significant application in the scaling and testing of OWC devices in order to include the effect of air-compressibility inside the chamber. Linear damping is here considered but the used of added chamber volume could also be applied for the more usual orifice type PTO simulant.

### *D. Hydrodynamic Performance*

In order to evaluate the effect of volumetric changes of the OWC air chamber on the hydrodynamic performance of the model scale OWC device, the non-dimensional capture width was derived for all test cases to form the plot displayed in Fig. 8. Analysing Fig. 8, we can observe the performance response curve typically associated with an isolated bent duct type OWC device, where the peak performance output occurs at the resonance frequency of the device [24-26], which is approximately 0.65 Hz for this particular test configuration. As the incident wave frequency moves away either side of the resonance frequency, there is an observable decline in the performance of the device.

The difference in performance for the different additional air chamber volumes is here not conclusive. The node present around $f$ = 0.95Hz, as discussed in [22] for the isolated device, has a restraining influence on the effect of air-compressibility on the performance for this case. Further testing for different devices would be necessary.

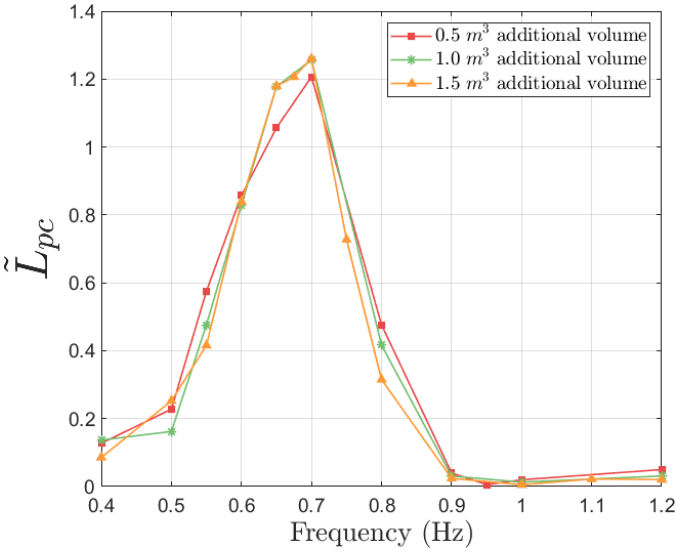


Fig. 8 Non-dimensional capture width of the OWC device for varying incident wave frequencies and volumetric air chamber variations.

## V. Conclusions

The purpose of this document was to present a preliminary investigation of the effect of air compressibility on a model scale experiment of an OWC device by scaling the chamber volume by the scale-factor (λ) squared instead of the typical (λ) cubed. Three different added chamber volumes were considered and their impacts on the pneumatic coefficients and hydrodynamic performance studied.

A recognisable phase shift between volume flux and pressure associated with air compressibility was identified as the air chamber volume was increased. The air compressibility coefficient, $\gamma_c$, was found to follow the theoretical trend as proposed in [1]. The $\gamma_c$ factor values obtained experimentally for the variations in $V_{0,c}$ remained relatively consistent across the test cases, yet varied in magnitude relative to the theoretical expression. Similarly, the newly derived expression was found to have a volume dependant factor $k$, which requires further investigation in future studies. The PTO coefficient , $\gamma_r$, was also found to be relatively constant over the frequencies as proposed in [1] but was however found to be dependent on the added volume.

The effects of air compressibility on the hydrodynamic performance here was not conclusive due to the natural behaviour of the device and will certainly require further testing.

This research presents a method with the potential for significant changes in the model scale investigation of OWC devices. The linear relationship established for the air compressibility coefficient provides a foundation that can be further developed toward more accurate assessments of full-scale OWC devices' hydrodynamic, pneumatic and energetic properties in experimental set-up.

## ACKNOWLEDGMENT

The authors acknowledge Mr. Daniel Male, Mr. Tim Lilienthal and Mr. Darren Young for their assistance regarding the design and construction of the experimental configuration. Without their expertise and guidance, this experimental investigation would not have been possible.

## REFERENCES

[1] Sarmento, A.J. and A.D.O. Falcão, "Wave generation by an oscillating surface-pressure and its application in wave-energy extraction," *Journal of Fluid Mechanics*, vol. 150, pp.467-485, 1985.

[2] Jefferys, R. and T. Whittaker, *Latching control of an oscillating water column device with air compressibility*, in *Hydrodynamics of Ocean Wave-Energy Utilization*. 1986, Springer. p. 281-291.

[3] Szumko, S., "Mechanical model for oscillating water column with compressibility," *Journal of Engineering Mechanics*, vol. 115, pp.1851-1866, 1989.

[4] Falcão, A.F.D.O. and P.a.P. Justino, "OWC wave energy devices with air flow control," *Ocean Engineering*, vol. 26, pp.1275-1295, 1999.

[5] Folley, M. and T. Whittaker. "The effect of plenum chamber volume and air turbine hysteresis on the optimal performance of oscillating water columns," in *Proceedings of 24th International Conference on Offshore Mechanics and Arctic Engineering*. 2005. Halkidiki, Greece: OMAE.

[6] Setoguchi, T., S. Santhakumar, H. Maeda, M. Takao, and K. Kaneko, "A review of impulse turbines for wave energy conversion," *Renewable Energy*, vol. 23, pp.261-292, 2001.

[7] Drew, B., A. Plummer, and M.N. Sahinkaya, "A review of wave energy converter technology," *Proceedings of the Institution of Mechanical Engineers, Part A: Journal of Power and Energy*, vol. 223, pp.887-902, 2009.

[8] Falcao, A.F.D.O., "Wave energy utilization: A review of the technologies," *Renewable and sustainable energy reviews*, vol. 14, pp.899-918, 2010.

[9] Lewis, A., S. Estefen, J. Huckerby, W. Musial, T. Pontes, and J. Torres-Martinez, *Ocean Energy. In IPCC Special Report on Renewable Energy Sources and Climate Change Mitigation [O. Edenhofer, R. Pichs-Madruga, Y. Sokona, K. Seyboth, P. Matschoss, S. Kadner, T. Zwickel, P. Eickemeier, G. Hansen, S. Schlömer, C. von Stechow (eds)]*, Cambridge University Press, Editor. 2011: Cambridge, United Kingdom and New York, NY, USA.

[10] Heath, T., "A review of oscillating water columns," *Phil. Trans. R. Soc. A*, vol. 370, pp.235-245, 2012.

[11] López, I., J. Andreu, S. Ceballos, I.M. De Alegría, and I. Kortabarria, "Review of wave energy technologies and the necessary power-equipment," *Renewable and Sustainable Energy Reviews*, vol. 27, pp.413-434, 2013.

[12] Delmonte, N., D. Barater, F. Giuliani, P. Cova, and G. Buticchi. "Oscillating water column power conversion: A technology review," in *2014 IEEE Energy Conversion Congress and Exposition (ECCE)*. 2014. IEEE.

[13] Ocean Energy Systems, *International Levelised Cost Of Energy for Ocean Energy Technologies*. Lisbon, Portugal: International Energy Agency 2015.

[14] Falcão, A.F. and J.C. Henriques, "Oscillating-water-column wave energy converters and air turbines: A review," *Renewable Energy*, vol. 85, pp.1391-1424, 2016.

[15] Ren21, *Renewables 2016 Global Status Report*. Paris: REN21 Secretariat 2016.

[16] Mankins, J.C., "Technology readiness levels," *White Paper, April*, vol. 6, pp.1995.

[17] Takahashi, S., H. Nakada, H. Ohneda, and M. Shikamori, "Wave Power Conversion by a Prototype Wave Power Extracting Caisson in Sakata Port," *Coastal Engineering*, vol. 23, pp.3440-3453, 1992.

[18] Torre-Enciso, Y., I. Ortubia, L. López De Aguileta, and J. Marqués. "Mutriku wave power plant: from the thinking out to the reality," in *Proceedings of the 8th European Wave and Tidal Energy Conference*. 2009. Uppsala, Sweden.

[19] Arena, F., V. Fiamma, V. Laface, G. Malara, A. Romolo, A. Viviano, G. Sannino, and A. Carillo. "Installing U-OWC devices along Italian coasts," in *32nd International Offshore Mechanics and Arctic Engineering Conference*. 2013. San Diego, USA: ASME.

[20] Arena, F., A. Romolo, G. Malara, and A. Ascanelli. "On design and building of a U-OWC wave energy converter in the Mediterranean Sea: a case study," in *32nd International Offshore Mechanics and Arctic Engineering Conference*. 2013. San Diego, USA: ASME.

[21] Arena, F., G. Malara, and A. Romolo, *A U-OWC wave energy converter in the Mediterranean Sea: Preliminary results on the monitoring system of the first prototype*, in *Renewable Energies Offshore*. 2015, CRC Press. p. 417-421.

[22] Howe, D. and J.-R. Nader, "OWC WEC integrated within a breakwater versus isolated: Experimental and numerical theoretical study," *International Journal of Marine Energy*, vol. 20, pp.165-182, 2017.

[23] Howe, D., J.-R. Nader, J. Orphin, and G. Macfarlane. "The Effect of Lip Extrusion on Performance of a Breakwater Integrated Bent Duct OWC WEC," in *European Wave and Tidal Energy Conference*. 2017. Cork, Ireland.

[24] Orphin, J., J.R. Nader, I. Penesis, and D. Howe. "Experimental Uncertainty Analysis of an OWC Wave Energy Converter," in *Proceedings of 12th European Wave and Tidal Energy Conference*. 2017. Cork, Ireland.

[25] Allsop, W., T. Bruce, J. Alderson, V. Ferrante, V. Russo, D. Vicinanza, and M. Kudella, "Large scale tests on a generalised oscillating water column wave energy converter," vol. 2014.

[26] Fleming, A., G. Macfarlane, S. Hunter, and T. Denniss. "Power Performance Prediction for a Vented Oscillating Water Column Wave Energy Converter with a Unidirectional Air Turbine Power Take-off," in *European Wave and Tidal Energy Conference*. 2017. Cork, Ireland.

[27] Fleming, A.N. and G.J. Macfarlane, "Experimental flow field comparison for a series of scale model oscillating water column wave energy converters," *Marine Structures*, vol. 52, pp.108-125, 2017.

[28] Mitchell Ferguson, T., I. Penesis, G. Macfarlane, and A. Fleming, "A PIV investigation of OWC operation in regular, polychromatic and irregular waves," *Renewable Energy*, vol. 103, pp.143-155, 2017.

[29] Day, S., I. Penesis, A. Babarit, A. Fontaine, Y. He, M. Kraskowski, M. Murai, F. Salvatore, and H. Shin. "Specialist Committee on Hydrodynamic Testing of Marine Renewable Energy Devices: final report and recommendations to the 27th ITTC," in *27th International Towing Tank Conference*. 2017.

[30] Nader, J.-R. "Hydrodynamic analysis and performance of a single fixed circular OWC device," in *Proceedings of the 11th European Wave and Tidal Energy Conference*. 2015. Nantes, France.

[31] Nader, J.-R., S.-P. Zhu, and P. Cooper, "Hydrodynamic and energetic properties of a finite array of fixed oscillating water column wave energy converters," *Ocean Engineering*, vol. 88, pp.131-148, 2014.

[32] Elhanafi, A., G. Macfarlane, A. Fleming, and Z. Leong, "Scaling and air compressibility effects on a three-dimensional offshore stationary OWC wave energy converter," *Applied Energy*, vol. 189, pp.1-20, 2017.

[33] Fleming, A., I. Penesis, L. Goldsworthy, G. Macfarlane, N. Bose, and T. Denniss, "Phase Averaged Flow Analysis in an Oscillating Water Column Wave Energy Converter," *Journal of Offshore Mechanics and Arctic Engineering*, vol. 135, pp.9, 2013.

[34] Fleming, A., I. Penesis, G. Macfarlane, N. Bose, and S. Hunter, "Phase averaging of the velocity fields in an oscillating water column using splines," *Proceedings of the Institution of Mechanical Engineers, Part M: Journal of Engineering for the Maritime Environment*, vol. 226, pp.335-345, 2012.

[35] Ferguson, T.M., G. Macfarlane, A. Fleming, and I. Penesis, "PIV investigation of 3-dimensional flow within an oscillating water column," *International Journal of Marine Energy*, vol. 11, pp.120-131, 2015.

[36] Ferguson, T.M., I. Penesis, G. Macfarlane, and A. Fleming, "A PIV investigation of OWC operation in regular, polychromatic and irregular waves," *Renewable Energy*, vol. 103, pp.143-155, 2017.